Available online at www.sciencedirect.com
ScienceDirect
Applied Surface Science 254 (2008) 4297–4302
applied surface science
www.elsevier.com/locate/apsusc

The iron oxidation state in Mg–Al–Fe mixed oxides derived from layered double hydroxides: An XPS study

M. Hadnadjev [a], T. Vulic [a], R. Marinkovic-Neducin [a], Y. Suchorski [b,*], H. Weiss [b]

[a] University of Novi Sad, Faculty of Technology, Bul. Cara Lazara 1, 21000 Novi Sad, Serbia
[b] Otto-von-Guericke-Universität, Chemisches Institut, Universitätsplatz 2, 39106 Magdeburg, Germany

Available online 19 January 2008

Abstract

Mixed oxides with large surface area and high thermal stability can be obtained by thermal treatment of the layered double hydroxides (LDH). Mg–Al–Fe mixed oxide samples with varying Mg/Al ratio and 5 mol.% of Fe were prepared in this way and the iron oxidation state (Fe_{ox}) in these compounds was studied by X-ray photoelectron spectroscopy (XPS), using a calibration based on the relation of Fe_{ox} to the splitting between the O 1s and Fe $2p_{3/2}$ centroids. The XPS results confirm Fe^{3+} as a dominant oxidation state in the studied mixed oxides. A vacuum-induced reduction of iron in the Fe_2O_3 and Mg–Al–Fe oxide samples has been observed and an influence of the Mg:Al ratio on this effect in mixed oxides has been detected. The role of the local variations of the electron density distribution in the close neighbourhood of the surface oxygen atoms in the mixed oxides in the reduction processes is discussed.

Keywords: X-ray photoelectron spectroscopy; Layered double hydroxides; Mixed oxides; Iron oxide

1. Introduction

Layered double hydroxides, LDHs, also often named ''anionic clays and hydrotalcite like materials'', are inorganic lamellar compounds with the general chemical formula: $[M_{1-x}^{2+}M_x^{3+}(OH)_2]^{x+}(A_{x/n}^{n-})\cdot mH_2O$, where M^{2+} and M^{3+} are divalent and trivalent metal ions, and x is the ratio $M^{3+}/(M^{2+} + M^{3+})$. M^{2+} and M^{3+} ions with ionic radii close to that of Mg^{2+} are accommodated in the brucite-like layers consisting of edge-sharing octahedral units which are stacked one on top of the other. The charge-compensating anions A^{n-} are, in turn, located in the interlamellar region [1–5]. The reason why LDHs are also known as hydrotalcite-like compounds lies in their structural similarity to hydrotalcite ($Mg_6Al_2(OH)_{16}CO_3\cdot 4H_2O$), a mineral that was first reported by Hochstetter [6] in 1842 and synthesized 100 years later by Feitknecht [7].

Usually, Cu, Fe, Mg, Mn or Ni are used as divalent and Co, Al, Mn, Fe, Ni or Cr as trivalent cations. This allows to tailor the LDH properties, using these different M(II) and M(III) ions, M(II)/M(III) ratios, and interlayer anions. The inhomogeneous charge distribution in such layered solids caused by partial isomorphous substitution of Mg^{2+} cations by e.g. Al^{3+} cations can be intentionally varied and may lead to interesting properties which are important in practical applications as catalysts (after calcination), catalyst supports, anion exchangers, polymer stabilizers, adsorbents, fillers (stabilisers for polymers), etc. [1,2]. A large number of LDHs has been studied in the last decades, both experimentally [3–5] and theoretically [8], thus establishing correlations between the structural parameters, formation energies and chemical composition of these compounds.

During the thermal treatment of an LDH its layered structure can collapse and mixed oxides with large surface area and higher thermal stability can be formed. In general, LDH phase synthesis is considered to be possible in the range $0.1 < x < 0.5$; the single-phase LDH synthesis is limited to $0.2 \leq x \leq 0.33$ [3,4]. Structure and surface properties of LDHs and derived mixed oxides depend strongly on the extent of M(III) substitution, chemical composition, and synthesis procedures.

It is also possible to synthesize an LDH outside of the optimum x range with the intention to form complex multi-phase oxides after thermal treatment. In this way structural

* Corresponding author. Tel.: +49 391 67 18 824.
E-mail address: Yuri.Suchorski@OvGU.de (Y. Suchorski).

0169-4332/$ – see front matter © 2008 Elsevier B.V. All rights reserved.
doi:10.1016/j.apsusc.2008.01.063

defects and contacts between oxide phases may be generated, resulting in metastability which can be of interest in catalysis. This was done in the present study in which aluminium was isomorphically substituted by iron in order to obtain redox properties necessary for catalytic reactions such as the nitrous oxide removal. The Fe oxidation state in complex multi-phase oxides derived from thermally activated Mg–Al–Fe layered double hydroxides has been studied by X-ray photoelectron spectroscopy (XPS), and the influence of the Mg/Al ratio on the reduction behaviour of the FeO_x component in the multiphase oxides was investigated using ultra high vacuum (UHV) as reductive environment.

2. Experimental

Low supersaturation coprecipitation with constant pH was used for the synthesis of LDH materials, following Ref. [9]. Mg–Al–Fe samples were prepared with different Mg/Al ratio (varying from 0.15 to 0.7) and with 5 mol.% of Fe. The $Mg(NO_3)_2$, $Al(NO_3)_3$ and $Fe(NO_3)_3$ solutions were continuously (4 ml/min) added maintaining constant pH (9.6–9.9) with simultaneous addition of NaOH and Na_2CO_3 solution. The precipitates were calcined for 5 h at 500 °C in air.

The XPS experiments were performed in an UHV multipurpose surface analysis system (SPECS, Germany) operating at base pressures $<10^{-10}$ mbar. For the XPS analysis the mixed oxide motes and Fe_2O_3 powder used as a reference material were compression-moulded in an almost optically dense ''powder monolayer'', fixed on the molybdenum sample holder and transferred under nitrogen to UHV. Since the vacuum-induced reduction of the LDH samples was studied in the present experiments, a fast sample transfer of less than 5 min between the start of the evacuation of the load lock and the first XPS spectrum at a pressure better than 5×10^{-9} mbar was necessary and accomplished [10].

A conventional X-ray source (XR-50, SPECS, Mg-K_α, 1253.64 eV and Al-K_α, 1486.65 eV) was used in a ''stop-and-go'' mode in order to reduce possible damage due to sample irradiation. The survey XP spectra and detailed high-resolution spectra (pass energy 10 eV, step size 0.1–0.2 eV) were recorded at room temperature with a hemispherical energy analyzer (PHOIBOS-150, SPECS), which provides the possibility of simultaneous photoelectron detection on nine channels, and allows fast data acquisition times (0.5 s per data point) with satisfactory signal-to-noise ratio. The binding energies for the Fe_2O_3 samples were corrected for charging effects by assuming a binding energy of 529.9 eV for the O 1s peak (529.86 eV, 529.92 eV and 529.84 eV were reported for FeO, Fe_3O_4 and α-Fe_2O_3, respectively [11]).

3. Results and discussion

The evaluation of chemical shifts in the binding energies (BEs) of photoelectrons originating from the same energy level but in different environments, detected over 40 years ago [12], is a widely used method for the determination of oxidation states of metals in their oxides. However, for many oxides, the use of XPS is complicated by the fact that the data analysis is often not unambiguous: as was shown in the calculations of multiplet structure of core p-vacancy levels, it is not always possible to use one and the same lineshape for fitting peaks of different oxidation state like $Me^{+,2+,3+}$, etc. [13,14]. The often ignored Fermi level shifting due to the oxygen vacancy defect concentration and final state effects contribute to the interpretation problems for many metal oxides [15]. These difficulties are also present for mixed oxides, where the situation becomes even more complicated since even the interpretation of the BE shifts of the O 1s XP line is controversial for such compounds [16].

For vanadium oxides, an independent method was proposed which is based on the evaluation of the splitting between the O 1s and V $2p_{3/2}$ centroids [15]. Such a splitting is not influenced by changes in the lineshapes caused by the lifting of degeneracy of sublevels in the 2p component due to interaction of the core-holes created by the photoemission process with the valence holes [13,14]. The calibration curve obtained in Ref. [15]

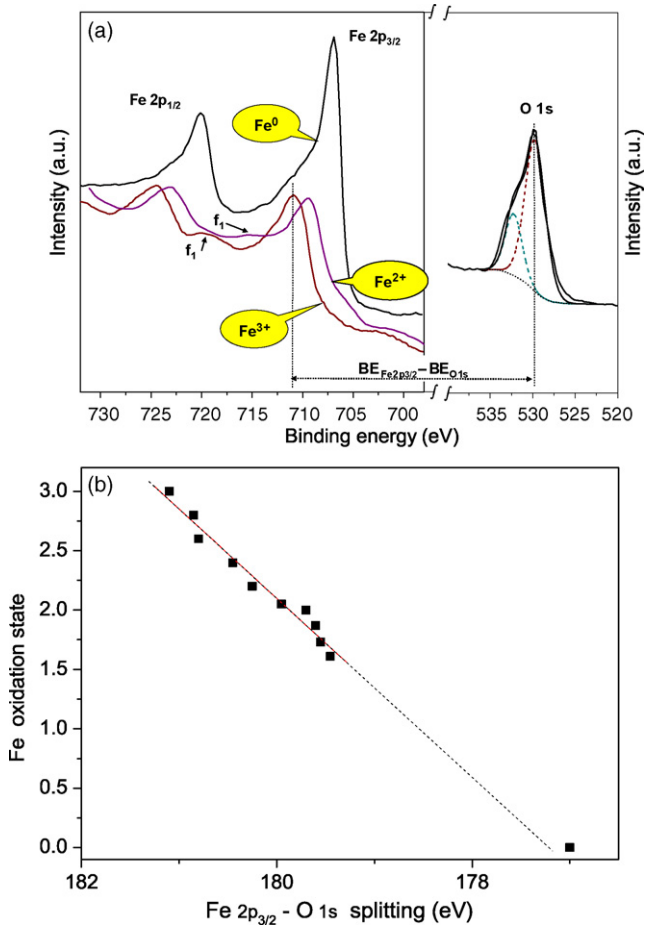

Fig. 1. Calibration of the iron oxidation state: (a) high-resolution photoelectron spectra for pure Fe_2O_3 (Fe^{3+}, lowest spectrum), an intermediate compound after prolonged Ar^+ sputtering, corresponding to Fe^{2+}, and metallic Fe (an Ar-sputtered iron foil, upper spectrum). The right-hand part shows the O 1s region, the splitting between the O 1s and Fe $2p_{3/2}$ peaks ($BE_{O\,1s} - BE_{Fe\,2p_{3/2}}$) is schematically indicated. (b) Dependence of the average oxidation state of iron (Fe_{ox}) on the $BE_{O\,1s} - BE_{Fe\,2p_{3/2}}$ value. The first-order least squares fit yields the linear relation $Fe_{ox} = 0.754\ (BE_{O\,1s} - BE_{Fe\,2p_{3/2}}) - 133.54$ (BEs in eV).

associates V_{ox}, the formal (average) oxidation state of V in a VO_x compound, with the binding energy difference $BE_{O\,1s} - BE_{V\,2p_{3/2}}$ and is very helpful in the evaluation of the average oxidation state of V in VO_x and VPO-based catalysts [10,15].

In the present work, we apply a similar approach to the evaluation of the oxidation state of iron in the mixed oxides. A pure Fe_2O_3 powder sample was sputtered with 2.0 kV Ar^+ ions in order to achieve the reduction of iron due to the preferential sputtering of oxygen. The O/Fe ratio measured at different intermediate stages of this process was compared to the initial O/Fe ratio and related to the $BE_{O\,1s} - BE_{Fe\,2p_{3/2}}$ splitting (Fig. 1a and b). Although such a sputtering procedure may create a depth profile of various oxidation states, the close similarity of the effective attenuation length for Fe 2p and O 1s photoelectrons allows an averaging across a depth profile caused by Ar^+ sputtering and thus a correct determination of the average stoichiometry. The lowest average oxidation state of iron of 1.6 achieved in the present experiments is in agreement with the results published in the literature, where a saturation of about 1.6 has been reported for Ar^+ sputtering of hematite (Fe_2O_3) powder [17].

From these calibration measurements the relation between Fe_{ox} and the $BE_{O\,1s} - BE_{Fe\,2p_{3/2}}$ splitting for FeO_x was obtained, with the result of a linear correlation (Fig. 1b), similarly as it was in the VO_x case for V_{ox} as a function of the $BE_{O\,1s} - BE_{V\,2p_{3/2}}$ splitting [15]. The positions of the Fe $2p_{1/2}$ (722.9 eV) and Fe $2p_{3/2}$ (709.6 eV) peaks (Fig. 1a) for an intermediate compound that corresponds to $Fe_{ox} = 2$ read from the calibration curve in Fig. 1b are in agreement with known values for FeO (722.7 eV and 709.7 eV, respectively [11]). The characteristic broad shake-up satellite (feature f_1 in Fig. 1a) at ~720 eV for $Fe_{ox} = 3$ and at ~716 eV for $Fe_{ox} = 2$, known for Fe 2p spectra for Fe_2O_3 and FeO, respectively [18,20], is also well visible in Fig. 1a. It is satisfying to notice that the extrapolation of the linear dependence in Fig. 1b towards $Fe_{ox} = 0$ provides a binding energy for Fe^0 close to that of metallic iron (706.9 eV were obtained for an iron foil in the present measurements, in quantitative agreement with literature data [11,18]). For such a fictitious splitting, the constancy of the O 1s peak position known for various FeO_x [11] was assumed also for $x \to 0$. Of course, the legitimacy of this extrapolation is questionable since it would require such a constancy of the O 1s level also at initial stages of iron oxidation, but nevertheless it can be interpreted as an indication of the validity of Hartree–Fock theory as applied to the XP process (see e.g. Ref. [19]).

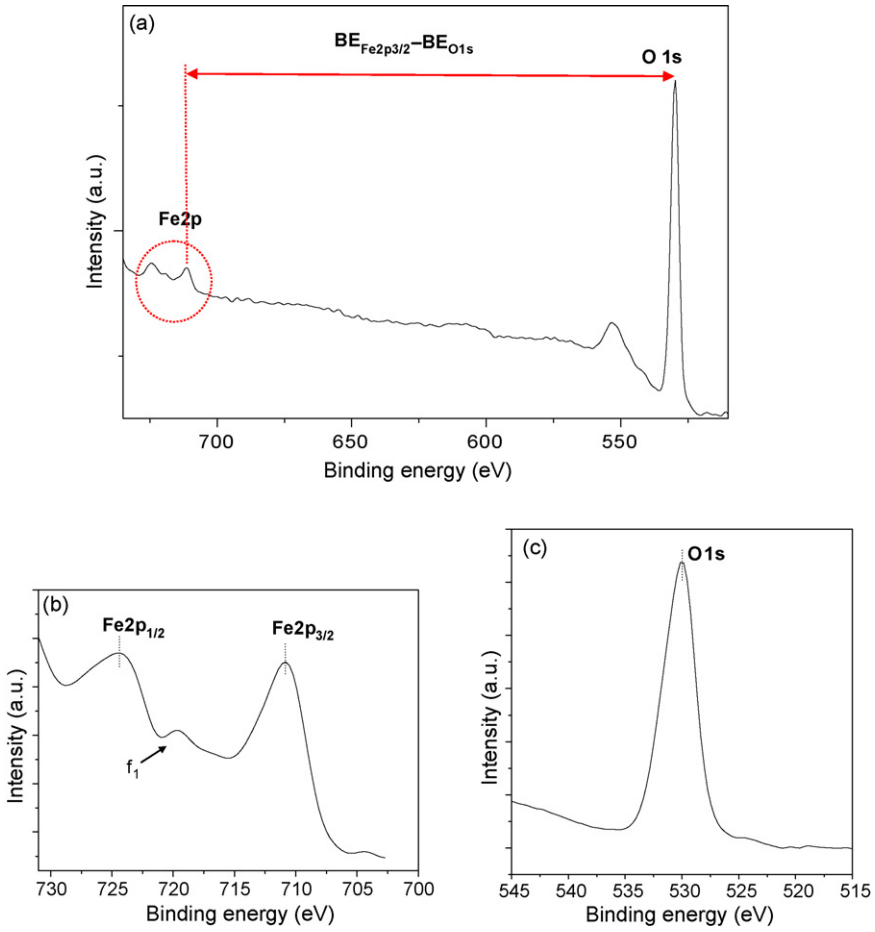

Fig. 2. (a) Section of the survey XP spectrum for a Mg–Al–Fe mixed oxide showing the splitting between the O 1s and Fe $2p_{3/2}$ peaks and demonstrating the Fe 2p to O 1s signal relation. (b) High-resolution Fe 2p spectrum for the same sample. All the characteristic features of the corresponding Fe^{3+} reference spectrum (see Fig. 1a) inclusive the satellite f_1 are present. (c) High-resolution O 1s spectrum for the same sample. The peak maximum position (530.0 eV) corresponds to that of the substitutional oxygen in Fe_2O_3 (529.9 eV, Fig. 1a).

The above calibration was performed for the iron oxides only, thus its applicability to mixed oxides has to be proven. Fig. 2a shows a section of the survey spectrum for a Mg–Al–Fe mixed oxide sample which contains only 5% of Fe, as illustrated by the low level of the Fe 2p XP signal in comparison to the O 1s peak. The $BE_{O\,1s} - BE_{Fe\,2p_{3/2}}$ splitting of 181.9 eV (see Fig. 2b and c) provides, via the calibration curve in Fig. 1b, an oxidation state $Fe_{ox} = 3$ for iron in this compound. Independently, the charge-effect correction based on the weak adventitious carbon 1s signal at 284.5 eV places the O 1s signal at 530.0 eV, Fe $2p_{1/2}$ at 724.3 eV, and Fe $2p_{3/2}$ at 710.9 eV, respectively. This is in a quantitative agreement with our measurements of Fe^{3+} in Fe_2O_3 (Fig. 1a) and with the corresponding literature data [11,17,20]. The presence of the satellites characteristic for Fe^{3+} in the Fe 2p spectra (feature f_1 in Fig. 2b, compare with Fig. 1a) additionally supports this independent evaluation. Thus the applicability of the Fe_{ox} calibration via the splitting of the Fe 2p and the O 1s peaks is demonstrated, at least for the present type of mixed oxides in which the position of the O1s peak is apparently not significantly influenced.

For all measured samples with different iron content, the initial $BE_{O\,1s} - BE_{Fe\,2p_{3/2}}$ splitting ranges between 180.9 eV and 181.2 eV, revealing thus an iron oxidation state $Fe_{ox} \approx 3$ in the studied Mg–Al–Fe mixed oxides. An independent evaluation based on the positions of the Fe $2p_{1/2}$ and Fe $2p_{3/2}$ peaks and their satellites confirms this conclusion.

It should be noted that the evaluation based on the splitting of metal and oxygen photoelectron peaks provides reliable results only in the case of ''normal ionic oxides'' (according to the classification proposed by Barr [21]) where the oxygen ion may be approximated by a more or less spherical shape. In the case of a pronounced polarization of its valence electronic shell, as in e.g. Ga oxides, the O 1s signal may have a more complicated, non-singular character [16]. In this case the ''splitting''-based estimation can become difficult. However, the deconvolution of the O 1s peak might help to distill the ''normal ionic'' component within the BE range of 530 ± 0.4 eV [21], which is useful at least for a semi-qualitative estimation of the average iron oxidation state.

The determination of an oxidation state of a cation in its oxide using conventional XPS, i.e. performing the measurements under

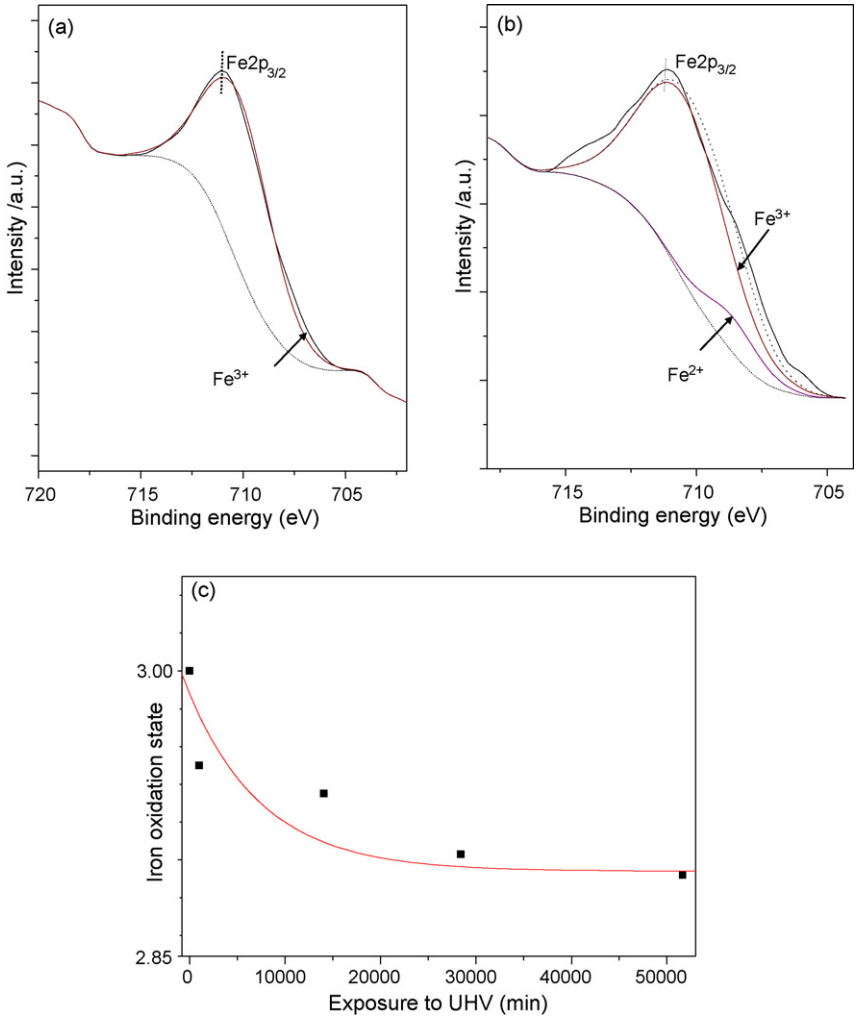

Fig. 3. (a) High-resolution Fe 2p spectrum for a Mg–Al–Fe mixed oxide sample with a Mg:Al ratio of 0.46 after 5 min exposure to UHV. Only the Fe^{3+} component is present. (b) The same, but after ~52,000 min in UHV. A Fe^{2+} contribution is clearly visible. (c) Evolution of the average oxidation state of iron during the long-term exposure to UHV.

UHV conditions, bears always the risk of a vacuum-induced reduction of the oxide samples. Such an effect was e.g. observed for vanadium oxides [10,22] and for vanadium phosphorus oxide (VPO) catalysts [10]. On the one hand, one can take precautions by using a "fast-transfer" technique, thus minimizing the exposure of the sample to UHV, on the other hand the observation of such a vacuum-induced reduction may provide interesting data about the reducibility of the oxide-based catalysts [23]. In order to prove the UHV-induced reduction of Mg–Al–Fe mixed oxides, the time evolution of the iron oxidation state in two samples with different Mg:Al ratios at constant content of Fe (5%) was monitored by XPS for a period of 36 days.

Fig. 3 shows the Fe $2p_{3/2}$ regions of the XP spectra for a sample with a Mg:Al ratio of 0.46, measured after 5 min and after ~52, 000 min of exposition to UHV, respectively. The corresponding deconvolution shows the appearance of the Fe^{2+} component (compare Fig. 3a and b) which is in accord with the shift of the Fe $2p_{3/2}$ peak maximum. The latter allows an independent estimation of the vacuum-induced changes in the iron oxidation state, using the calibration curve in Fig. 1b.

The comparison of the reduction behaviour of samples with different Mg:Al ratios seems to reveal a significant role of the Mg:Al ratio in the vacuum-induced reduction of iron in the mixed oxides: while for a sample with a Mg:Al ratio of 0.46 a remarkable reduction of iron has been observed (Fig. 3c), an only marginal effect (within the error limits), if at all, was observed for a sample with a much higher Mg:Al ratio of 8.5. At the present stage of the study it is difficult to distinguish between the different possible contributions, i.e. if either Mg plays a stabilising or Al a promoting role in this reduction process. However, it seems to be clear that the local electronic environment around the oxygen ion is responsible for an eased release of oxygen. Since the oxygen release takes place via the surface sites, the surrounding Mg or Al surface atoms may be interpreted to a certain (very simplified) degree as a kind of coadsorbed species. In this case it is clear, that the local electron density distributions in the close vicinity of Mg and Al surface atoms differ significantly, thus unequally influencing the bonding of the neighbouring oxygen atoms.

It is interesting to prove the reducibility of pure Fe_2O_3 under similar UHV conditions. The corresponding deconvolution of

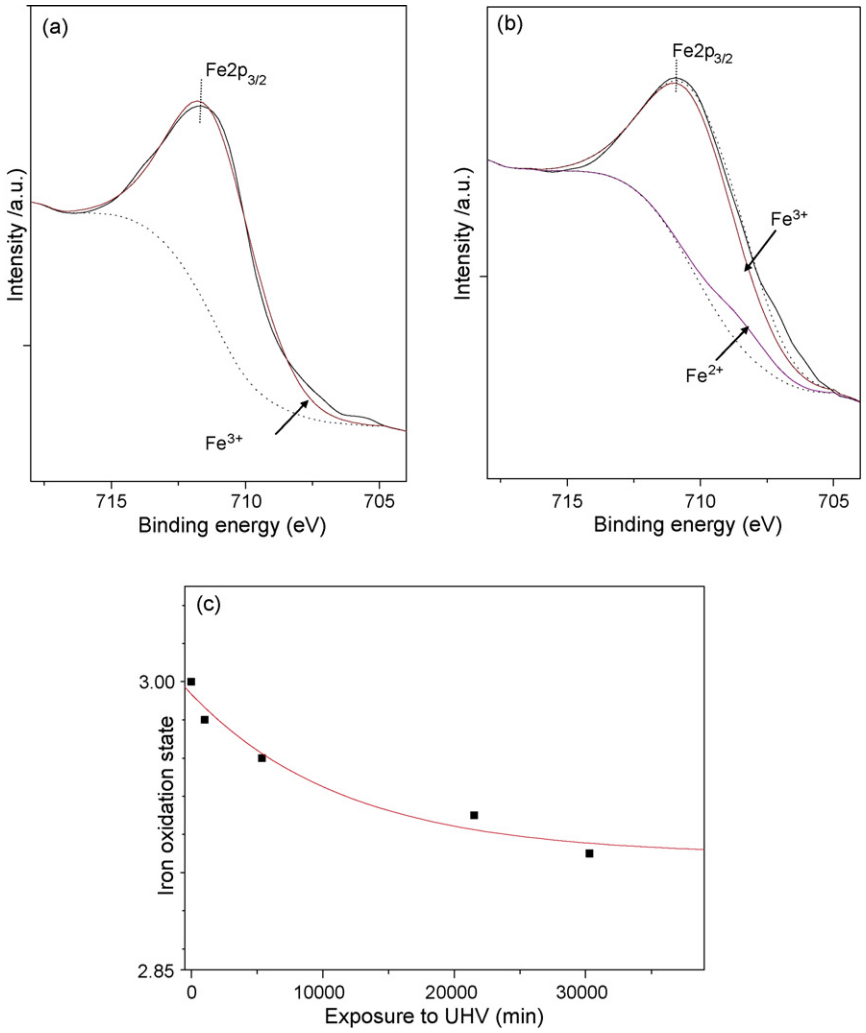

Fig. 4. (a) High-resolution Fe 2p spectrum for a Fe_2O_3 oxide sample after 5 min exposure to UHV. Only the Fe^{3+} component is present. (b) The same, but after ~30,000 min in UHV. (c) Evolution of the average oxidation state of iron upon prolonged exposure to UHV.

the Fe $2p_{3/2}$ peak of a Fe_2O_3 sample, subjected to a long-term exposition to UHV, and the time evolution of Fe_{ox} are shown in Fig. 4a–c, correspondingly. In this case, the vacuum-induced reduction appears to be similar to that observed for the mixed oxide with a lower Mg:Al relation. This result suggests that mixed oxides with a higher content of cations of oxidation state +3 are easier reducible than those with cations of oxidation state +2. In future kinetic studies the temperature and the metal components will be varied. This may allow to get a deeper insight into the mechanism of oxygen release and oxygen diffusion which presumably limits the reduction rate.

4. Summary

The splitting between the O 1s and Fe $2p_{3/2}$ peaks in the XP spectra serves as a reliable and independent measure of the average iron oxidation state in FeO_x and ionic Fe-containing mixed oxide compounds with an O 1s peak of a singular structure. The XPS analysis confirms Fe^{3+} as the main oxidation state of iron in the mixed oxides, which are derived from the layered double hydroxides. A long-term exposition of the FeO_x and Mg–Al–Fe oxide samples to UHV leads to a vacuum-induced reduction of iron in which the Mg:Al ratio plays an important role: in the mixed oxide case, the samples with a lower Mg:Al ratio appear to be less stable in UHV with respect to the iron oxidation state, i.e. they are easier reducible. The peculiarities of the local electron density distribution in the close neighbourhood of the surface oxygen atoms influenced by surrounding Fe, Mg and Al atoms seem to affect the reducibility of iron in the mixed oxides.

Acknowledgements

M.H. acknowledges financial support by the Serbian Ministry of Science and Environmental Protection (Contract no. OI 142024) and by the German Academic Exchange Service (DAAD).

References

[1] A. de Roy, C. Forano, J.P. Besse, in: V. Rives (Ed.), Layered Double Hydroxides: Present and Future, Nova Science Publishers, New York, 2001, pp. 1–37.
[2] S.P. Newman, W. Jones, in: W. Jones, C.N.R. Rao (Eds.), Supermolecular Organisation and Material Design, Cambridge University Press, Cambridge, 2002, pp. 295–331.
[3] A. Vaccari, Catal. Today 41 (1998) 53.
[4] X. Duan, D.G. Evans, Layered Double Hydroxides. Structure and Bonding, Springer, Berlin, 2006.
[5] J.J. Bravo-Suárez, E.A. Páez-Mozo, S.T. Oyama, Quím. Nova 27 (2004) 601.
[6] C. Hochstetter, J. Prakt. Chem. 27 (1842) 375.
[7] W. Feitknecht, Helv. Chim. Acta 25 (1942) 131.
[8] A. Trave, A. Selloni, A. Goursot, D. Tichit, J. Weber, J. Phys. Chem. B 106 (2002) 12291.
[9] W.T. Reichle, Solid States Ionic 22 (1986) 135.
[10] Y. Suchorski, L. Rihko-Struckmann, F. Klose, Y. Ye, M. Alandjiyska, K. Sundmacher, H. Weiss, Appl. Surf. Sci. 249 (2005) 231.
[11] P. Graat, M.A.J. Somers, Surf. Interface Anal. 26 (1998) 773, and references therein.
[12] K. Siegbahn, C. Nordling, A. Fahlman, R. Nordberg, K. Hamrin, J. Hedman, G. Johansson, T. Bergmark, S.E. Karlsson, I. Lindgren, B. Lindberg, Nova Acta Regiae Soc. Sci. 4 (1967) 20.
[13] R.P. Gupta, S.K. Sen, Phys. Rev. B 10 (1974) 71.
[14] R.P. Gupta, S.K. Sen, Phys. Rev. B 12 (1975) 15.
[15] G.W. Coulston, E.A. Thompson, N. Herron, J. Catal. 163 (1996) 122.
[16] D.A. Pawlak, I. Masahiko, O. Masaoki, K. Shimamura, T. Fukuda, J. Phys. Chem. B 106 (2002) 504.
[17] K.R. Rhodes, Modern Microsc. 2 (2006) 27.
[18] K. Wandelt, Surf. Sci. Rep. 2 (1982) 1.
[19] M. Cardona, L. Ley, in: M. Cardona, L. Ley (Eds.), Topics in Applied Physics, vol. 26, Springer, Berlin, 1978.
[20] P. Graat, M.A.J. Somers, Appl. Surf. Sci. 100/101 (1996) 36.
[21] T.L. Barr, Modern ESCA: The Principles and Practice of X-ray Photoelectron Spectroscopy, CRC Press, Boca Raton, 1994.
[22] M. Heber, W. Grünert, J. Phys. Chem. B 104 (2000) 5288.
[23] F. Klose, T. Wolff, H. Lorenz, A. Seidel-Morgenstern, Y. Suchorski, M. Piórkowska, H. Weiss, J. Catal. 247 (2007) 176.